Transactions, SMiRT-22
San Francisco, California, USA - August 18-23, 2013
Division X

BEHAVIOR AND DESIGN OF SC COMPOSITE WALLS FOR ACCIDENT THERMAL LOADING

Amit H.Varma[1], Kadir C. Sener[2] and Derek Winkler[3]

[1] Assoc. Professor, School of Civil Eng., Purdue University, West Lafayette, IN (ahvarma@purdue.edu)
[2] Ph.D. Candidate, School of Civil Eng., Purdue University, West Lafayette, IN (ksener@purdue.edu)
[3] Senior Engineer, URS Corporation, Denver, CO, (derek.winkler@urs.com)

ABSTRACT

Pressurized water reactor (PWR) nuclear power plant containment structures are designed withstand to accidental thermal loading scenarios that would initiate due to a pipe breakage that carry high pressure water at elevated temperatures. Experimental tests have been performed in order to determine the effects of accidental thermal loading on the flexural and shear strength and stiffness of SC composite walls. This paper summarizes the experimental findings obtained from the tests on beam specimens that were subjected to combination of thermal heating and out of plane loading. The objectives of this paper are to provide recommendations for analysis and design of SC walls subjected to combined thermal and mechanical loads using previous analytical and experimental research.

INTRODUCTION

The objective of the accident thermal + out of plane shear tests was to experimentally investigate the flexural and out-of-plane shear behavior of a typical SC wall subjected to nonlinear thermal gradients. Additionally, to confirm that the resulting thermal cracking in concrete can be estimated conservatively using the equations developed for ambient conditions.

The effects of elevated temperatures on the steel material properties (E_s and F_y) and concrete material properties (E_c and f'_c) are accounted using Table NA-4.2.1 and NA-4.2.2 in AISC N690-12 (2012). As stated in the commentary of AISC N690-12, the stress-strain response of steel at elevated temperatures is more nonlinear than at room temperature and experiences less strain hardening.

At elevated temperatures the deviation from linear behavior is represented by the proportional limit, F_p(T), and the yield strength, F_y(T), is defined at a 2% strain. The surface temperature to be applied to the heated zone is determined to be 450 °F (232 °C). At 450 °F, the yield F_y(T), and ultimate strength, F_u(T), remains same to its values at ambient temperature, and the proportional limit F_p(T) occurs at 75% of the yield strength F_y(T), Finally, mechanical properties of steel and concrete at 450 °F are given in Table 1. However, it should be noted that the thru-depth temperature distribution decays rapidly from the heated steel surfaces. Therefore, temperatures that the concrete portions see are much less than the surface temperature (450 °F).

Table 1 - Properties of Steel and Concrete at Elevated Temperature

Steel Properties at 450 °F	$k_E = E(T)/E = G(T)/G$	$k_p = F_p(T)/F_y$	$k_y = F_y(T)/F_y$
	0.87	0.75	1.0
Concrete Properties at 450 °F	$k_c = f'_c(T)/ f'_c$	$E_c(T)/E_c$	$\varepsilon_{cu}(T)$,%
	0.89	0.70	0.5

The SC walls consist of thick concrete walls with steel faceplates on the exterior surfaces acting as reinforcement. The steel faceplates are made from A572 Gr. 50 steel and anchored to the concrete infill typically using A108 steel headed shear studs. The exterior steel faceplates are connected to each other through the concrete using rectangular tie bars made from A572 Gr.50 steel. The headed shear stud diameter and spacings are designed so that the interfacial shear strength of the SC walls is greater than the out-of-plane shear strength of SC walls.

Accident thermal loading subjects SC walls to heating from both sides, and results in similar temperatures on the two exterior steel faceplates. The difference between thermal properties (conductivity and specific heat) of steel and concrete causes a significant thermal lag to occur in the concrete infill. The results of heat transfer analyses indicate nonlinear (parabolic) temperature profiles through the composite cross-section, which result in cracking of the concrete infill of SC walls.

EXPERIMENTAL RESEARCH

In a previous research performed by the authors (2011) with one sided 3-hour long heating at 300 °F surface temperature and 10 psi initial mechanical loading, it was shown that the out-of-plane shear strength of SC walls under accident thermal loading has not resulted in significant difference on the shear and flexural strength capacities. The concrete cracking in this accident thermal loading condition did not have a major influence on the out-of-plane shear strength of SC beams. This was credited mostly to the thermally induced cracks that are perpendicular to the steel plates which occurred while exposed to combination of the heating and mechanical loading. These cracks had to turn by 45-60º to develop out-of-plane shear cracks in the concrete, which takes approximately the same amount of force (V_c) as that required to develop new shear cracks due to the anisotropic cracking nature of concrete. Additionally, the steel shear reinforcement (V_s) contribution to the out-of-plane shear strength is unchanged because the temperature of the steel shear reinforcement embedded in the concrete is not high enough to change the mechanical properties, such as the yield strength.

In summary, previous experimental research indicates that the SC wall design capacities were not expected to be significantly reduced due to accident thermal loading conditions. These design capacities under accident thermal loading for the walls are be confirmed by the following tests. Therefore the design equations developed for ambient conditions are recommended for usage

Similar to the previous experimental research, in the current experimental program two specimens were tested by subjecting them to heating followed by four-point bending in the out-of-plane direction. However this time the surface temperature and the initial mechanical loading pressure magnitudes were increased to study the effects, where the steel surface temperature was increased to 450°F and the initial pressure loading to 40 psi. Both specimens have shear span a/d ratios equal to 2.0, where *a* is the shear span length and d is the wall thickness. The shear reinforcement plates are spaced at equal distance in the length direction of the beam specimens. For demonstrating the effects of thermal loading more clearly, identical specimens were tested by subjecting them to only monotonically increasing mechanical loading as control specimens.

(i) Specimen T1 was heated in the uniform moment region (mid-span) to confirm the effects of accident thermal loading on flexural capacity. The specimen is large scale and an identical specimen without heating is tested. The flexural yielding of the steel plates is expected to be the governing limit state, and the section will have ductile behavior when subjected to out-of-plane loading. The thermal frame was placed between the two loading frames to apply heating to the constant moment region.

(ii) Specimen T2 was heated in one of the uniform shear region to confirm the effects of accident thermal loading on out-of-plane shear strength. It is known from previous experimental research that the SC wall specimens exhibit non-ductile failures under shear loading. One of the shear spans of the specimen loaded in four-point bending was heated, which allowed focusing on one side and observing the failure mode in detail during the test. The layout for the thermal and mechanical loading frames is shown in Figure 2.

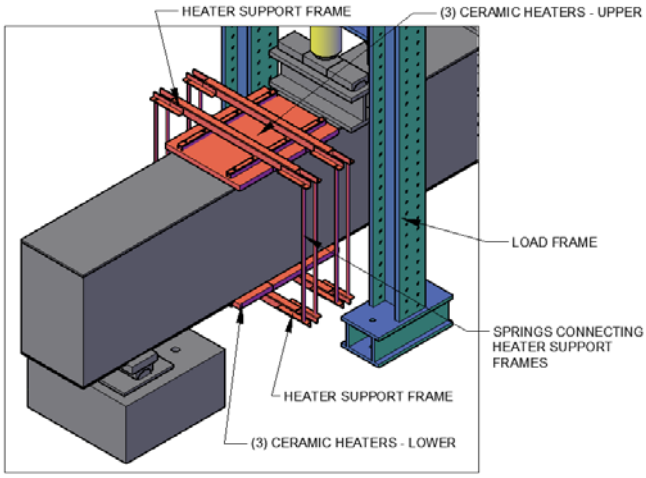

Figure 1 - Out-of-plane Shear + Thermal Loading Test Schematic Sketch

Testing Approach

The accident thermal + out-of-plane shear tests were conducted by subjecting each specimen to a combination of heating and monotonically increasing loads at two load points. To apply the thermal loading, heaters were placed on the opposing steel faceplates, and insulating materials were provided between the faceplate and heaters. The applied temperatures were controlled using thermocouples attached to the outside surfaces of the steel plates. This allowed for direct measurement of the steel faceplate temperature. The exposed surface time-temperature curve was controlled by the thermal controller and data acquisition system, which was independent of the remaining thermocouples and data acquisition system instrumentation system.

The thermal loading and mechanical loading was applied as follows:

Step 0. Out-of-plane loading simulating the shear force corresponding to 40 psi pressure was applied first. A loading-unloading-reloading cycle was conducted at this load level. The applied loading is maintained constant until the end of Step 1.

Step 1. The temperature of the steel faceplates was increased gradually to 450°F in approximately 20 minutes. The steel faceplate temperatures were maintained for approximately 3 hours for each specimen.

Step 2. The out-of-plane loading was increased to 60% of the calculated load capacity for each specimen and a loading-unloading-reloading cycle is conducted at this level while maintaining the heating. The load capacity of the specimens were estimated using the commonly used design equations that are adopted by the industry. It is common to estimate the out-of-plane shear strength of SC walls using the ACI 349 shear strength equation for reinforced concrete members. Similarly for bending moment strength the JEAC equation is widely adopted mainly due its simplicity. The conservatism of usage of both equations for SC walls are previously shown by the authors (Varma et. al. 2011). The equations are given below; the shear strength equations are given in Equations 1 thru 3, and the flexural strength is given in Equation 4.

$$V_n = V_c + V_s \quad \text{Equation 1}$$

$$V_c = 2\sqrt{f`_c} \cdot A_c \ \text{(psi)} \quad \text{Equation 2}$$

$$V_s = A_v \cdot F_{y.sh} \cdot \frac{T}{s} \quad \text{Equation 3}$$

$$M_n = A_{pl} \cdot F_{y.pl} \cdot \frac{7}{8} T \quad \text{Equation 4}$$

In these equations; f'_c is the compressive strength of concrete, A_c is the cross-sectional area of concrete, $F_{y.sh}$ is the yield strength of the vertical shear reinforcement, A_v is the cross-sectional area of shear reinforcement, $F_{y.pl}$ is the yield strength of steel faceplate, A_{pl} is the cross-sectional area of steel faceplate on one side, T is the section depth, and s is the shear reinforcement spacing.

Step 3. The out-of-plane loading was increased monotonically to failure, while maintaining the heating.

Measured Material Properties

The concrete used for accident thermal + out of plane shear tests were obtained from a local concrete vendor. Specimen T1 had a maximum aggregate size of 3/4in, and Specimen T1 had a maximum aggregate size of 3/8in. The day of test concrete compressive strengths were measured based on testing at least three concrete cylinders; where the strength for Specimen T1 was 5880 psi and for Specimen T2 was 6920 psi.

The certified mill test reports (CMTR) for the steel plates used for the faceplates and tie bar plates, and the results of tensile testing performed in accordance with ASTM E8 for commercial grade dedication (CGD) of the studs were submitted. These CMTRs and CGD test results indicate that the face plate and shear reinforcement plates had an average of 60 ksi yield strength and the shear studs having a yield strength ranging at 55 ksi.

Sensor Instrumentation

The response of the specimens were monitored with several different type of instrumentation tools at several locations during each test. These instrumentations included displacement sensors, inclinometers, strain gauges and thermocouples.

Displacement sensors were at several locations along the length of the specimen to measure vertical deflections. Support settlements were also measured using displacement sensors to calculate the chord (net) vertical deflection. Additional displacement sensors were attached to the interface of concrete and steel plate to measure slip at the steel-concrete interface along the length. This information may be useful to establish the level of composite action exhibited in the test.

Inclinometer sensors were attached to the beam cross-sections at load and support locations. Additional inclinometers were attached at either side of the heated region to obtain the flexural stiffness in that region. The rotations measured under the load points allowed for the average curvature at mid-span to be calculated, which was used to develop moment vs. curvature plots for the SC beam cross-section. The support inclinometers will measure the rotations of the support and demonstrate that the cylindrical support bearings perform their functions adequately.

Steel strain gauges were attached on both top and bottom steel plates along the beam length. The steel plate strain gauges were aligned to be on the same cross-section to evaluate section strain diagrams. The data obtained from these gauges was also used to validate other findings obtained from different sensors, such as section stiffness (EI) obtained from the inclinometers (moment-curvature diagrams) or neutral axis location obtained from concrete gauges. High temperature strain gauges were used in the heated zone in order to be protected from temperature. Additionally, internal strain gauges were attached to tie bars and shear studs, which were later embedded in concrete. The tie bar strain gauges measured vertical strain at their mid-depth.

In order to monitor the temperature during the tests, Type K thermocouples were attached at various locations throughout the specimen. Type K thermocouples are capable of measuring temperatures in the range of -328° F to 2282°F (-200°C to 1250°C). Thermocouples were welded to the outer steel plate surfaces, the tie bars, and the shear studs in order to measure the steel temperatures. To measure the temperature throughout the depth of the concrete, a “thermocouple tree” was used. The tree consisted of a threaded rod with thermocouples welded along the length. The rod was positioned prior to casting the concrete and the rod and thermocouples were embedded in the concrete.

EXPERIMENTAL RESULTS

SPECIMEN T1

This specimen was heated in the uniform moment region (mid-span) to confirm the effects of accident thermal loading on flexural capacity. The thermal frame was placed between the loading frames to apply heating to the constant moment region as shown in Figure 2, depicted with the overall beam dimensions.

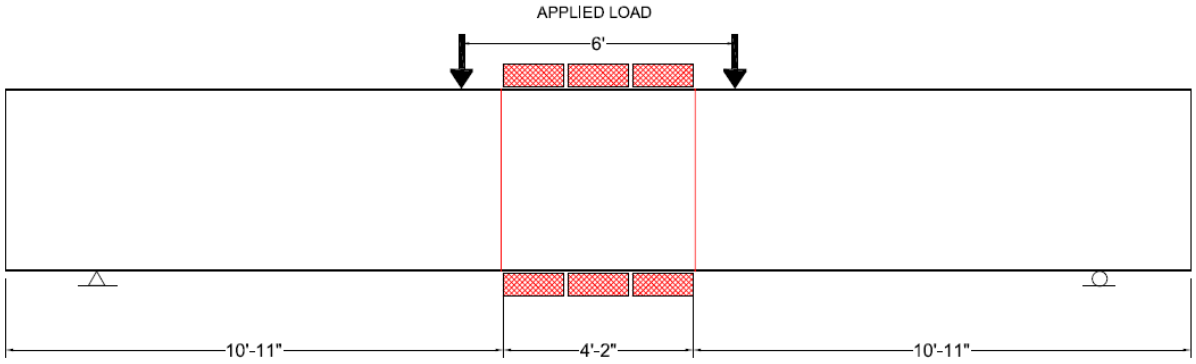

Figure 2 - Elevation View with Heaters of Specimen T1

Time histories for the applied temperature and the applied loading are shown in Figure 3. Before applying heating, the applied loads (mechanical loads) were gradually increased from zero to the shear force level that corresponds to 40 psi uniform pressure acting over the entire top surface of the beam. After the first load cycle, the mechanical loading was held to maintain a constant level of bending moment in the uniform moment region. The surface temperatures were increased as rapidly as possible from ambient to 450˚F. The surface temperature was then held constant at 450°F for two hours. Then the applied mechanical loads were increased gradually to the 60% of the calculated beam flexural capacity. Finally, the applied load was increased to the limit of the specimen while maintaining the surface temperature constant at 450°F.

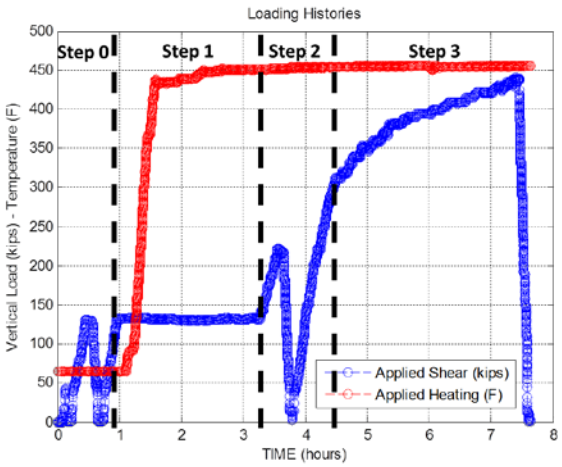

Figure 3 - Applied Load and Steel Plate Temperature Histories of Specimen T1

Thermally induced cracking occurred almost immediately following the onset of heating. These cracks were caused by differential thermal expansion of the steel and concrete, induced by the vertical temperature gradient extending through the section depth. The heating of the specimen also caused some moisture to escape through open cracks. Figure 4 shows thermal crack patterns on the west side of the specimen where vertical cracks were formed at 20 minutes of heating.

Mid Span – West Face

Figure 4 - Concrete cracking of Specimen T1 during heating

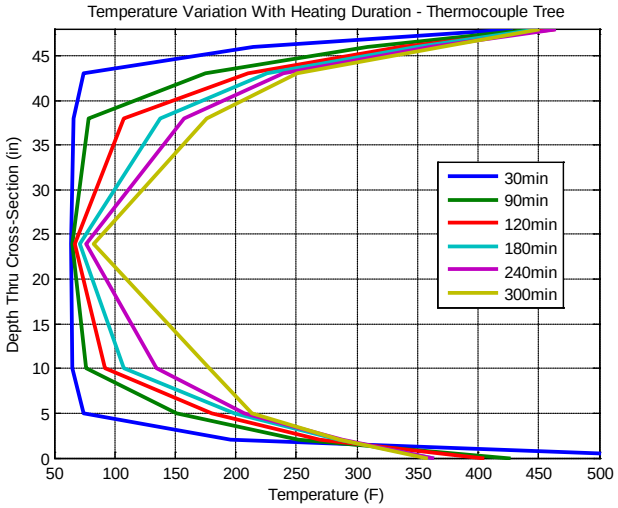

Figure 5 - Thru-depth temperature distributions obtained using the thermocouples on the thermocouple tree

Numerous cracks initiated at the top and bottom of the beam directly adjacent to the heated area and propagated through the center of the section as heating progressed. The heating has caused extension of existing vertical shrinkage as well as bending cracks that occurred after applying the load corresponding to the 40 psi uniform pressure.

Figure 5 illustrates a thermal distribution plot through the cross-section depth obtained by connecting the thermocouple tree measurements at different elevations at different times during testing. As can be observed in the figure that the temperature distribution shown by the thermocouple tree is close to symmetric. The tree was located near the center of the two operational heaters at the mid-span, so it was expected that the top and bottom portions of the temperature distribution would be similar.

The cross-section of the wall experienced a nonlinear thermal gradient and the faceplate steel experienced 450˚F as prescribed at the mid-span (middle of the center span) of Specimen T1. The specimen experienced concrete cracking, elevated steel temperature, and other affects that may impact the flexural strength of the specimen.

Figure 6 shows the average shear force on the shear spans versus the chord vertical mid-span deflection for the specimen. The force-displacement responses indicate an elastic/plastic response with significantly ductile response due to flexural yielding of the beam specimen. The transition from elastic response to yielding is smoother due to the changes in the steel yield strength at elevated temperature. The figure indicates that although the yielding initiates at a lower load level due to the change in the steel plate material properties at high temperature, the ultimate force was not less than what was achieved from the ambient case.

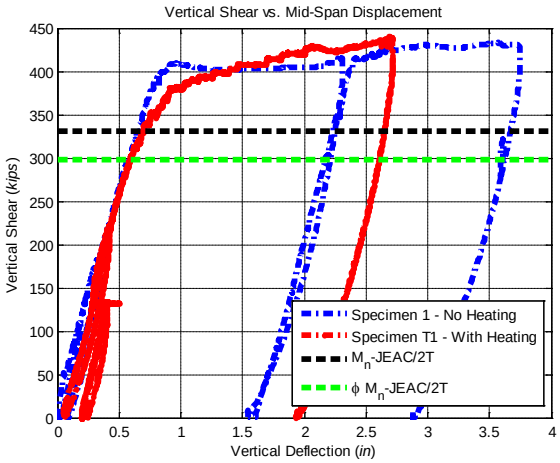

Figure 6 - Average load vs. average net mid-span deflection comparison of Specimen T1

The applied load increased gradually to maximum load level with the mid-span displacement reaching to three times of the displacement at yielding initiation. The experiment was terminated at this point because the actuator had reached its limiting stroke, and the behavior did not seem to indicate onset of brittle failure. The load displacement indicates some displacement creep in the heating step where the load was maintained at Step 1. In both the pre- and post-yielding region, there is some nonlinearity in the force-deflection response due to cracking of the concrete and hardening of the bottom steel plate.

The horizontal lines in the figure indicate the nominal and design flexural strength calculated by Equation 4, where the reduction factor (ϕ) for bending is used as 0.90. As shown, the specimen flexural strength is greater than that estimated conservatively by the design flexural strength equations provided by the JEAC equation. The nominal design flexural strength is shown to be less than the actual strength of the specimen with about 25% safety margin.

The section average moment-curvature response, where the curvature was estimated using the rotation measured by the rotation transducer located at both ends of the heated zones. The average curvature was equal to the difference between the rotations measured at the rotation transducers divided by the distance between the two sensors. The response is compared with the fiber section analysis that does not account for the heating. The initial stiffness of the specimen in this region follows the cracked transform section stiffness, as it compares well with the fiber model, which accounts for material non-linear behavior of both steel and concrete.

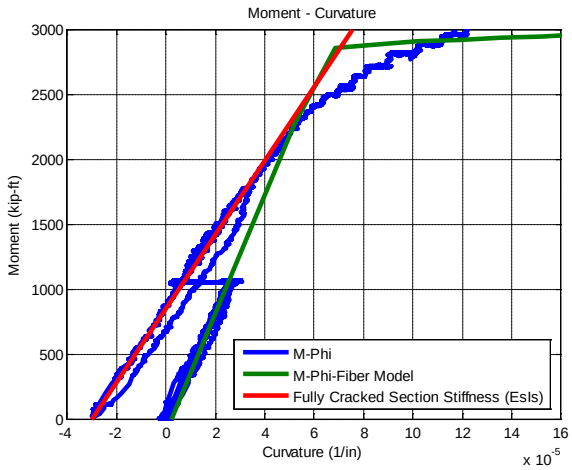

Figure 7 - Moment-curvature behavior of Specimen T1, zoom into initial loading stage

Heating is applied after the first load cycle which cracks the concrete and therefore the flexural stiffness slightly reduces. As shown in Figure 4, the through depth cracks that occurred due to the heating extinguished the concrete contribution to the flexural stiffness. Therefore the measured stiffness is equal to the fully cracked flexural stiffness that is calculated by considering only the steel portions (E_sI_s) but accounting for the heating effects. The steel modulus of elasticity is reduced to 87% of the ambient condition when exposed to 450F^o according to Table NA-4.2.1 of AISC N690-12 document.

SPECIMEN T2

This specimen was heated in the south shear span region to confirm the effects of accident thermal loading on out-of-plane shear strength. The shear force that corresponds to 40 psi uniform pressure in Step 0, initiated diagonal shear cracking in the shear spans and flexural cracks in both the shear span and mid-span regions at several locations along the length of the beam. The occurrence of the diagonal cracks was the main difference that was not seen in the previous experimental research by the authors (2011), where the initial loading was corresponding to 10 psi uniform pressure.

The diagonal shear cracks widened and extended in Step 1, where the heaters were turned on while the shear load was maintained on the specimens. Figure 9 shows a photo taken during Step 1 and indicates several diagonal cracks that formed and extended in the heating phase.

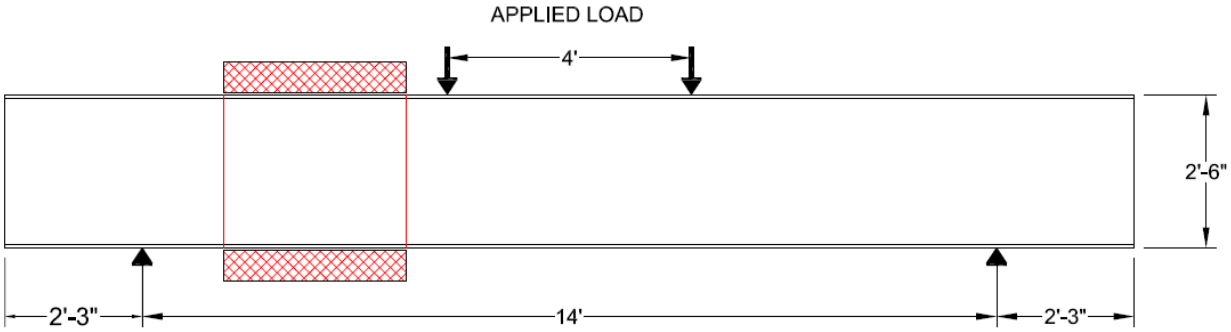

Figure 8 - Elevation View with Heaters of Specimen T2

Figure 9 - Diagonal Shear Crack Occurrence of in the heating phase

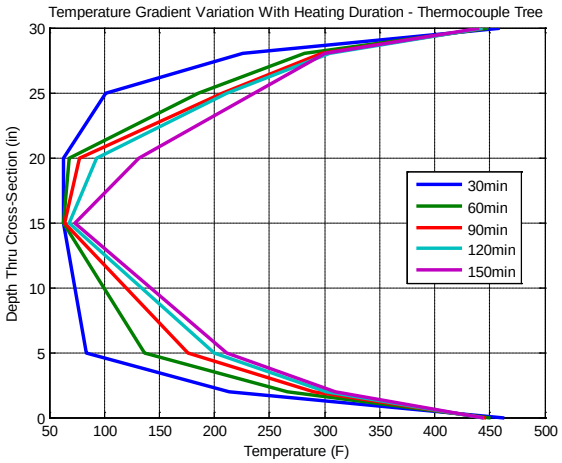

Figure 10 - Thru-depth temperature distributions obtained using the thermocouples on the thermocouple tree

Similar to the Specimen T1 test, thermally induced cracking occurred almost immediately after the onset of heating. These cracks were caused by differential thermal expansion of the steel and concrete caused by the vertical temperature gradient extending through the section depth. Therefore these vertical cracks also formed in the heated region that coincide with the diagonal cracks.

As shown in Figure 10, temperatures were measured on a thermocouple tree that was located in the centerline of the cross section of the specimen and the heater panels assemblies. Due to the two sided heating, the temperature distributions are symmetric per the section mid-depth similar to the previous test.

Figure 11 shows the average force versus vertical deflections for the specimen. In this figure, the average force is calculated by taking the average of the forces applied by the two hydraulic rams. The vertical deflections were measured from the chord of the specimen, which was estimated as the straight line defined by the support vertical displacements.

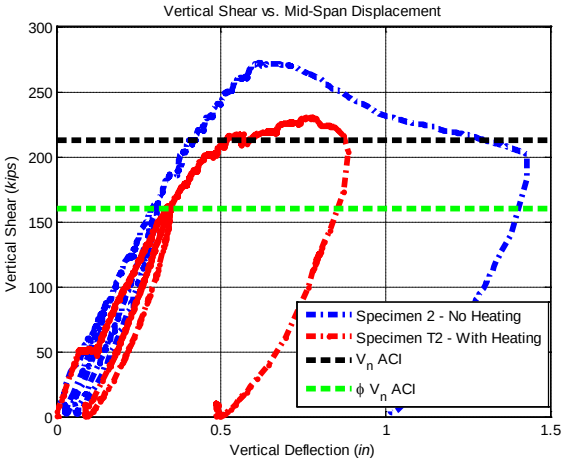

Figure 11 - Average load vs. average net mid-span deflection comparison of Specimen T2

The figure shows the average shear force versus average mid-span displacement comparison of identical specimens but one not having any thermal loading. As the heated specimen reached its peak load at a mid-span displacement that is similar to the ambient specimen, shear failure of the specimen occurred at this point, and the specimen started losing its load carrying capability from that point onwards to the unloading. The strain gauge measurements in both the heated and ambient test did not indicate measurements in the steel faceplates that are in excess of yield strain which confirmed that the failure mode was diagonal shear failure due to excessive cracking in concrete and yielding in the shear reinforcement plates.

The figure also indicates that the response of the heated specimen was slightly softer both in strength and stiffness. This was due to the additional diagonal cracks that formed by being subjected to a combination of heating and loading in Step 1. However, the nominal and design shear strengths calculated based on the measured material properties indicate that the equations can be used to conservatively estimate the strength, where the reduction factor (ϕ) for shear strength is used as 0.75.

As shown in the figure, the specimen shear strength is greater than that estimated conservatively by the design flexural strength equations. The design shear strength calculated using measured properties are less than the actual shear strength of the specimen, with about 20% safety margin.

The previous experimental research conducted by the authors on the out-of-plane shear strength of SC walls subjected to accident thermal load condition (2011) has shown that the strength is not diminished from the ambient condition. The reasoning for the different outcome obtained in this study was credited mainly to not forming any diagonal cracks in the initial load or the heating phase. It was observed in the previous experimental research that formation of diagonal cracks in the final loading stage required almost the same load demand as the ambient case. However, in the current loading condition, especially with a higher initial pressure level, the diagonal cracks are already formed at the end of Step 1.

Therefore, the concrete shear strength contribution vanished in this first loading and heating step. This observation is also supported by the fact that the maximum force level obtained from the heated and unheated test differ by approximately $1.3\sqrt{f`_c}\,A_c$, which is in a force range that is considered to be corresponding to the concrete diagonal cracking force by the reinforced concrete research community.

CONCLUSIONS AND RECOMMENDATIONS

Accident thermal loading causes a significant nonlinear thermal gradient to develop through the composite cross-section. The exterior steel faceplates are at the exposed (maximum) temperatures, and most of the concrete infill or core remains at relatively low temperatures. This nonlinear thermal gradient causes through section concrete cracking to occur at the heated sections. The material properties at the heated section are reduced due to elevated temperatures. The reduced material properties can be estimated using the elevated temperature material property Tables NA-4.2.1 and NA-4.2.2 in accordance with the AISC 690-12.

The flexural behavior of a member exposed to accident thermal heating is expected to be as follows: concrete cracking due to the nonlinear thermal gradient will initially cause the compressive force of the moment couple in the cross-section to be resisted by the compressive steel plate only. Measuring flexural stiffness values that are equal to flexural stiffness that assumes full concrete cracking supports this observation. The compressive steel plate has adequate slenderness/compositeness level to prevent local buckling before yielding. However, concrete crack closure will eventually occur as the moment demand (and the corresponding compressive force produced by the moment couple) becomes large. The final moment capacity will be governed by a stress state similar to the case for ambient temperature conditions and can be calculated conservatively using the equations derived for ambient case, such as the flexural strength equation provided by the JEAC code.

The accident thermal loading case has shown to reduce the shear strength by degrading the concrete contribution by forming and extending diagonal tension cracks in the heating phase. The formation of these cracks are a result of combined thermal and mechanical loading. In this current research the thermal and mechanical loading was increased in magnitude from a similar previous experimental program that was performed by the authors. The increase in these load intensities have allowed forming the diagonal cracks which diminished the concrete contribution. The reduction on the overall shear strength is also approximately equal to the force level that corresponds to concrete cracking. Nevertheless, the reduced out-of-plane shear strength due to the thermal loading can still be underestimated using the shear strength equations that are developed for the ambient loading case. This is due to the safety margin that is inherently provided in the ambient case equations, such as the ACI equation for shear strength of reinforced concrete beams.

Further experimental testing and calibrated 3D non-linear finite element analysis models are recommended with different combinations of initial heating and mechanical loading to provide additional insights into behavior and also to build additional confidence in the results to be used by designers.

REFERENCES

ACI 349 (2006), “Code Requirements for Nuclear Safety-Related Concrete Structures and Commentary,” American Concrete Institute, Farmington Hills, MI

JEAC 4618 (2009). “Technical Code for Seismic Design of Steel Plate Reinforced Concrete Structures: Buildings and Structures,” *Japanese Electric Association Nuclear Standards Committee*, Tokyo, Japan.

Specification for Safety-Related Steel Structures for Nuclear Facilities (ANSI/AISC N690-12),

Varma, A.H., Malushte, S.R., Sener, K., Booth, P.N., and Coogler, K. (2011c). “Steel-Plate Composite Walls: Analysis and Design Including Thermal Effects.” *Trans. of the Internal Assoc. for Struct. Mech. in Reactor Tech. Conf.*, SMiRT-21, Paper No. 761, New Delhi, India, Nov.6-11, 2011, IASMiRT, NCSU, Raleigh, NC.